AREAL CRATER DENSITY ANALYSIS OF VOLCANIC SMOOTH PLAINS: MARE IMBRIUM, A REVISED APPROACH. L. R. Ostrach[1,2] and M. S. Robinson[1], [1]School of Earth and Space Exploration, Arizona State University, Tempe, AZ; [2]NASA Goddard Space Flight Center, Greenbelt, MD. (lostrach@ser.asu.edu)

Introduction: The lunar maria were emplaced over an extended period of time [>2 Ga; e.g., 1–3], and mare units exhibit marked color differences in multispectral data that correlate with distinct mineralogical units and ages [e.g., 3–6]. In Mare Imbrium, emplacement occurred in three primary phases: older basalts exposed in the east are interpreted to be Imbrian in age, while the younger basalts in the west are Eratosthenian and late Imbrian in age [e.g., 5–10]. Absolute model age determination for units in Mare Imbrium [e.g., 4–8] relied on multispectral classification to distinguish geologic units, but not all planetary bodies exhibit multispectral differences within volcanic units (age and composition), as is the case on Mercury [e.g., 11–13].

Areal crater density (ACD) analysis was used as a novel approach to identify resurfacing boundaries within Mare Imbrium, as a test case for mercurian studies. Initial ACD analysis identified a boundary between two regional geologic units in Mare Imbrium [14] that corresponded to previously mapped and dated units [e.g., 5,7,8]. Here, subsequent refinements to methodology and expansion of the measurement area confirm previous findings [14], indicating that ACD measurements provide a reliable technique to distinguish relative ages among geologic units without employing spectral information.

Methods: LROC WAC 100 mpp monochrome mosaics [15] at high (75°) and low (57°) solar incidence angles and a 100 mpp Clementine UV-VIS ratio composite mosaic [e.g., 16] were used to expand the measurement area [14] within Mare Imbrium to encompass 2.27×10^5 km^2. This region contains strong spectral contrasts between two spatially expansive units and large published model age differences [5,8]. The spectral boundary was approximately centered within the count area to promote comparable sampling areas for ACD analysis. CraterTools in ArcMap [17] was used to measure craters with diameters (D) ≥0.5 km.

ACD was determined from a point density calculation using a moving neighborhood approach in ArcMap, and the center of each crater was represented as a point. The output cell size and neighborhood radius were user-defined, and application of a weighted edge correction minimized edge effects near measurement boundaries. Color classification was designated using Poisson probabilities (10th percentile). To establish where ACD values reflected real geologic differences as opposed to noise from small measurement numbers, synthetic ACD maps were generated from the crater measurements for (1) the entire study area (7100 points), to investigate regional variations, and (2) for each spectral unit (4900 and 2200 points for the spectrally red and blue units, respectively), to investigate the extent of local variation that is expected statistically within a geologic unit.

Results: From the crater measurements in Mare Imbrium, the absolute model age (AMA) is 3.3 ± 0.05 Ga for the spectrally red unit (~15–18 wt% FeO, ~2–5 wt% TiO_2 [18]) and 2.2 ± 0.16 Ga for the blue unit (~17–20 wt% FeO, ~7–10 wt% TiO_2 [18]). In the ACD map, two regional units are observed [**Fig. 1**], and examples of high, low, and moderate ACD are shown in **Fig. 2**. The regional units are separated by an irregularly shaped boundary extending approximately northwest to southeast that is similar to the compositional boundary observed in this region.

Synthetic ACD maps generated for the entire study area exhibit widespread intermediate values with localized high and low density regions distributed across the measurement area [**Fig. 3A**]. Synthetic ACD maps generated to investigate variation within the spectral units [**Fig. 3B**] reproduce the measured ACD results, and contain smaller regions of intermediate ACD within the high and low density regional units.

Discussion and Conclusions: ACD measurements within Mare Imbrium identify a regional boundary at the contact between two spectrally distinct regions with AMAs >300–500 my and spatial extents $>1 \times 10^4$ km^2 [**Fig. 1**]. Geologic units dated as older (3.2–3.6 Ga [5]; 3.0–3.3 Ga [8]) exhibit higher ACD (>35652 craters with D ≥0.5 km per 10^6 km^2) and younger units (2.0–3.0 Ga [5]; 2.2 Ga [8]) have lower ACD (<25974 craters with D ≥0.5 km per 10^6 km^2); the ACD results agree with other dating studies of this region [e.g., 7,9,10]. Furthermore, spectral units with AMA differences of several hundred million years [5] are not observed in the ACD map created here, suggesting that while the reported ages are statistically different, the ages may not be geologically meaningful. Thus, ACD measurements provide a reliable technique to distinguish relative ages among geologic units as well as a means to explore the statistical significance of published absolute model ages. Moreover, the ability to distinguish surface units of different ages from measures of crater frequencies in Mare Imbrium, when spectral information is not available or units do not exhibit spectral contrasts, shows that the ACD technique may be applied to other planetary bodies to search for age boundaries within contiguous smooth plains units. For example, multispectral differences within volcanic units are not observed on Mercury [e.g., 11–13], so the ACD method can be used to test hypotheses concerning timing of smooth plains emplacement [13].

References: [1] Hartmann W.K. et al. (1981) In: BVTP, 1049–1127. [2] Stöffler D. et al. (2006) Rev. Mineral. Geochem, 60, 519–596. [3] Hiesinger H. et al. (2011) Spec. Pap. – Geol. Soc. Am, 477, 1–51. [4] Pieters C.M. (1978) Proc. Lunar Plan. Sci. Conf, 9th, 2825–2849. [5] Hiesinger H. et al. (2000) J. Geophys. Res, 105, 29239–29275. [6] Staid M.I. and C.M. Pieters (2001) J. Geophys. Res, 106, 27887–27900. [7] Schaber G.G. et al. (1975) The Moon, 13, 395–423. [8] Bugiolacchi R. and J.E. Guest (2008) Icarus, 197, 1–18. [9] Schaber G.G. (1973) In: Apollo 17 PSR, NASA SP-330, 30–17 to 30–25. [10] Boyce J.M. and A.L. Dial Jr. (1975) Proc. Lunar Sci. Conf, 6th, 2585–2595. [11] Robinson M.S. et al. (2008) Science, 321, 66–69. [12] Denevi B.W. et al. (2009) Science, 324, 613–618. [13] Denevi B.W. et al. (2013) J. Geophys. Res, 118, 1–17. [14] Ostrach L.R. and M.S. Robinson (2013) Lunar Plan. Sci. Conf., 44th, abstract 1086. [15] Speyerer E.J. et al. (2011) Lunar Planet. Sci. Conf., 42nd, abstract 2387. [16] Belton, M.J.S. et al. (1992) Science, 255, 570–576. [17] Kneissl T. et al. (2011) PSS, 59, 1243–1254. [18] Lucey P.G. et al. (2000) J. Geophys. Res, 105, 20297–20306.

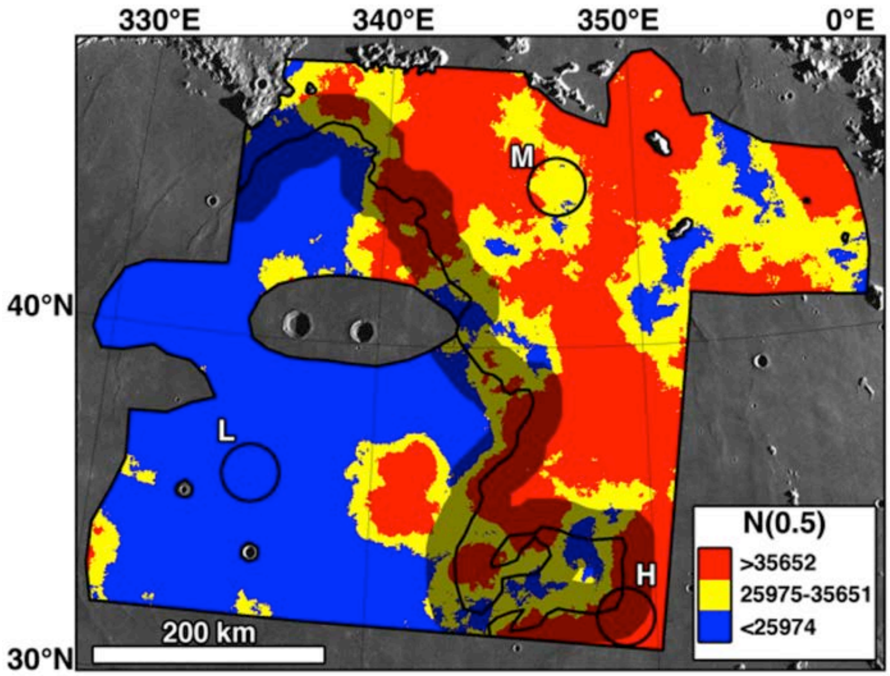

Fig. 1. ACD map derived from the measured crater population (D ≥0.5 km); output cell is 1 km and neighborhood radius is 25 km. The compositional boundary identified in multispectral data is observed (black line) with ±25 accuracy (grayed area; reflecting uncertainty resulting rom smoothing due to the technique), indicating the presence of two regional geologic units. ACD map overlaid on LROC WAC 75° incidence angle mosaic centered at 45.0°N, 340.0°E in Mare Imbrium.

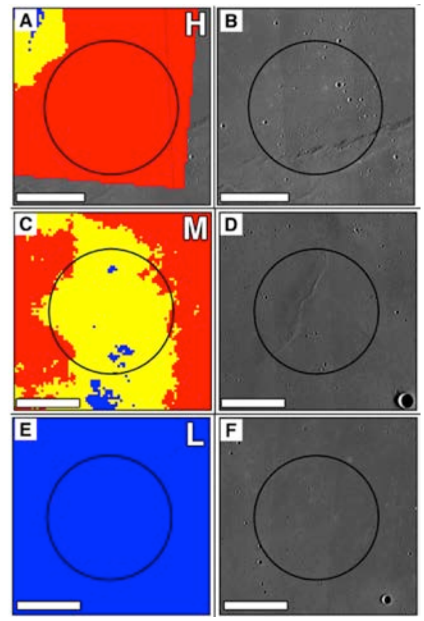

Fig. 2. Example neighborhood ACD (radius 25 km; Fig. 1). Selection from (A,B) the high (H) density region; (C,D) the moderate (M) density region; and (E,F) the low (L) density region. ACD map on left with color classification from Fig. 1, LROC WAC 75° incidence angle mosaic on right; scale bar is 25 km.

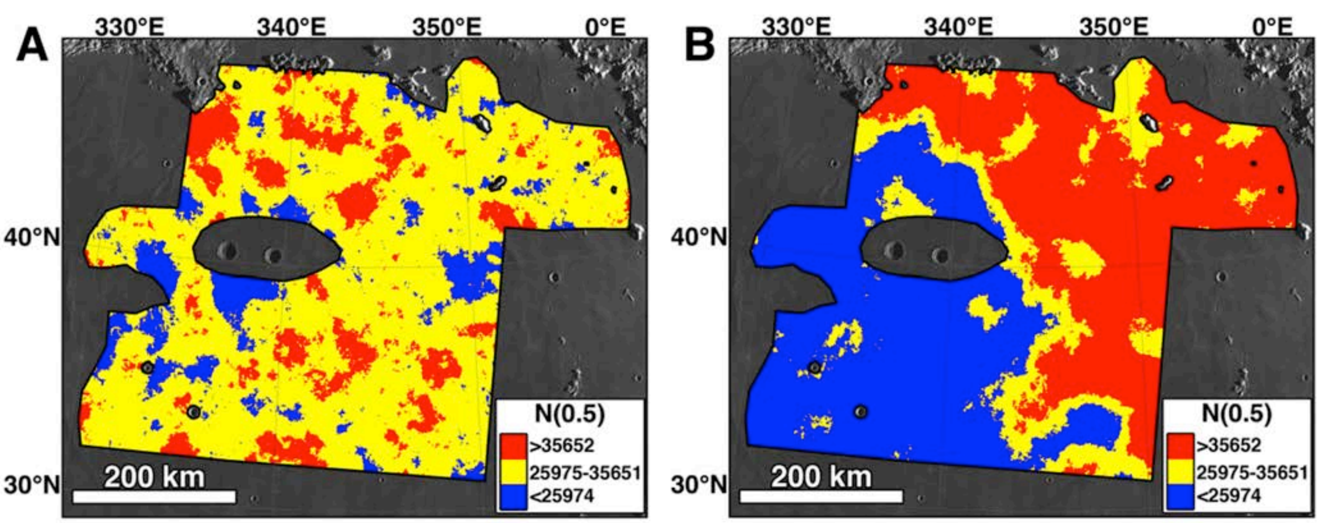

Fig. 3. Synthetic ACD maps generated from random point distributions. (A) Synthetic ACD map generated for one regional unit, indicating that the observed ACD map (Fig. 1) contains statistically significant variation within the measured crater population and that the observation of two units reflects a real age difference between crater populations. (B) Synthetic ACD map generated for two units, indicating that within the observed regional units in Fig. 1, some ACD variation is attributed to real ACD differences (e.g., surface modification due to ejecta emplacement, non-obvious secondary contamination) and not statistical noise.